Supplementary Information

Gas sensors based on the oxide skin of liquid indium

Xiangyang Guo,[a] Chung Kim Nguyen,[a] Aishani Mazumder,[a] Yichao Wang,[ab] Nitu Syed,[ae] Enrico Della Gaspera,[c] Torben Daeneke,[a] Sumeet Walia,[a] Samuel J. Ippolito,[a] Ylias M. Sabri,[a] Yongxiang Li,*[a] Ali Zavabeti*[ad]

[a.] *School of Engineering, RMIT University, Melbourne, VIC, 3000, Australia. Email: yongxiang.li@rmit.edu.au and ali.zavabeti@rmit.edu.au*
[b.] *School of Life and Environmental Sciences, Deakin University, Waurn Ponds, Victoria 3216, Australia*
[c.] *School of Science, RMIT University, Melbourne, VIC, 3000, Australia.*
[d.] *Department of Chemical Engineering, The University of Melbourne, Parkville, Victoria 3010, Australia, Email: ali.zavabeti@unimelb.edu.au*
[e.] *School of Physics, The University of Melbourne, Parkville, Melbourne, Victoria 3010, Australia*

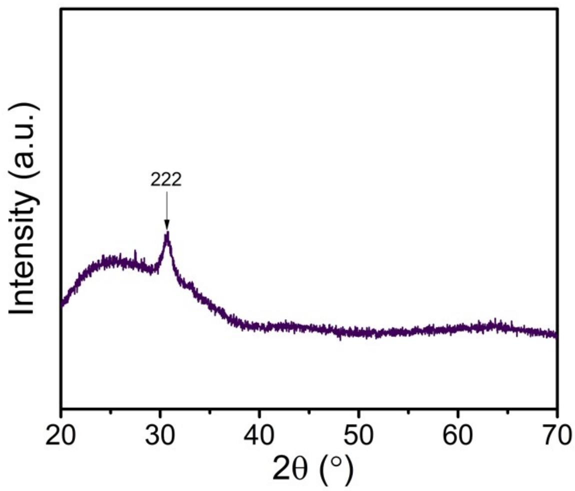

Supplementary Figure S1. XRD pattern of multi-transferred In_2O_3 on glass substrate.

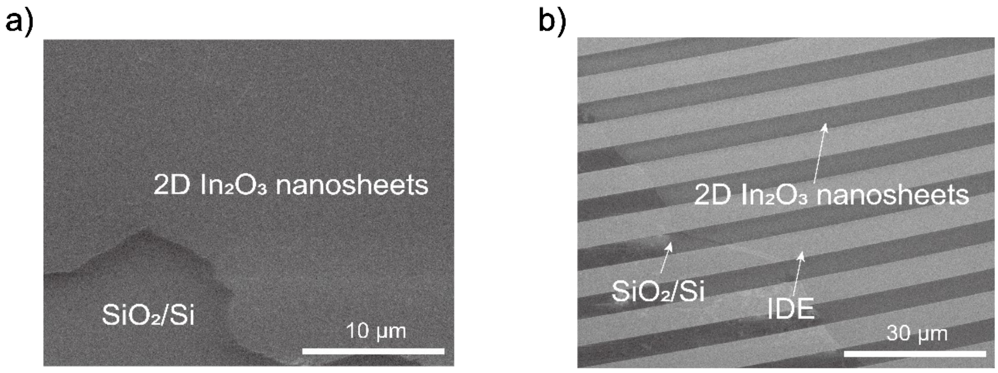

Supplementary Figure S2. The SEM images of 2D In_2O_3. a) A SEM image of 2D In_2O_3 nanosheets on SiO_2/Si substrate. b) A SEM image of 2D In_2O_3 nanosheets on IDEs.

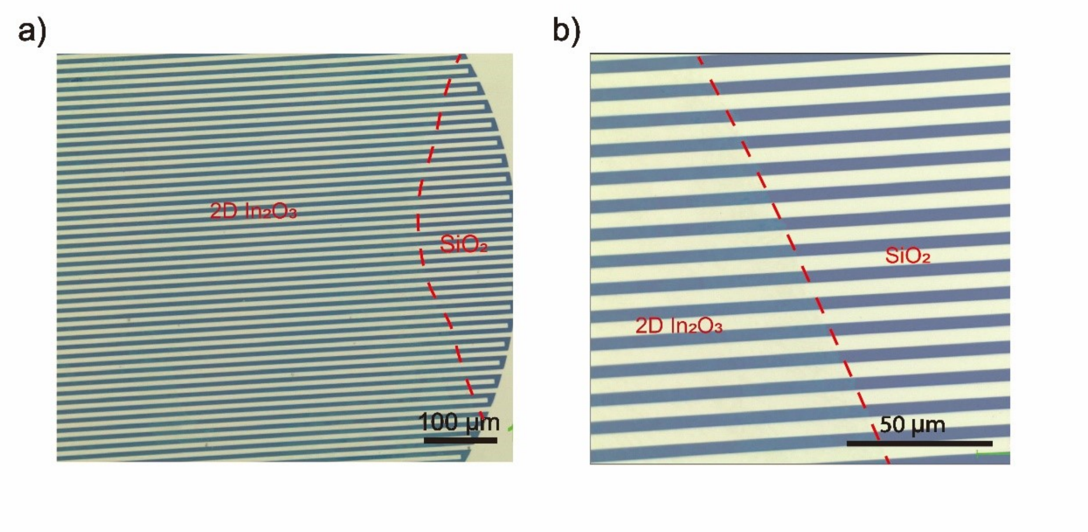

Supplementary Figure S3. The optical images of 2D In_2O_3 nanosheets on IDEs at different magnifications.

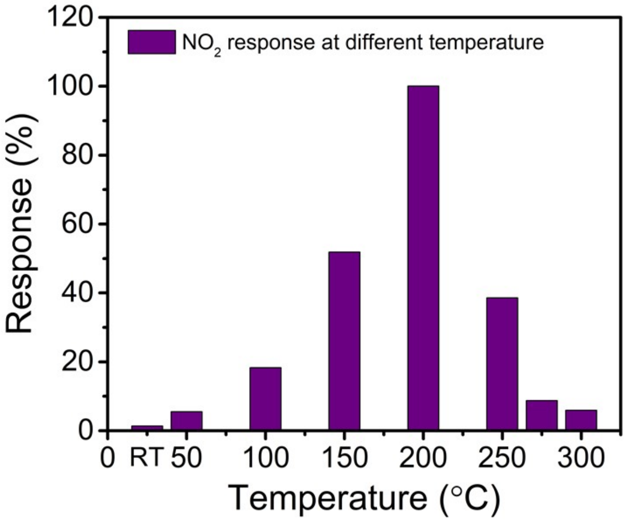

Supplementary Figure S4. Optimization of 2D In_2O_3 response to NO_2 against temperature.

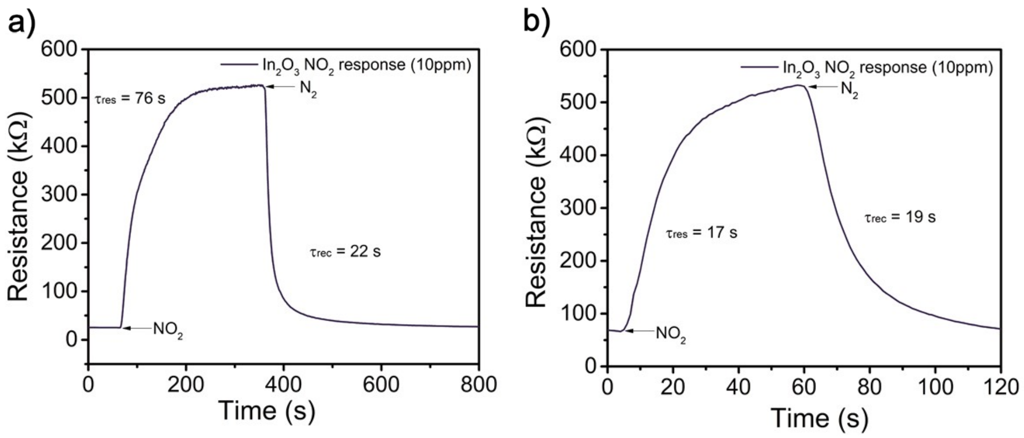

Supplementary Fig. S5. Response-recovery of 2D In_2O_3 gas sensors to 10 ppm NO_2 at 200 ℃ under steady-state and transient conditions. a) Steady-state response-recovery cycle of 2D In_2O_3 gas sensors to 10 ppm NO_2 in 5 min in NO_2 and 10 min in N_2. The response of 1974 %. b) Transient response of 700 % to 10 ppm NO_2 in 1 min in NO_2 and 1 min in $N_{2,}$ showing practical response-recovery times of less than 20 s.

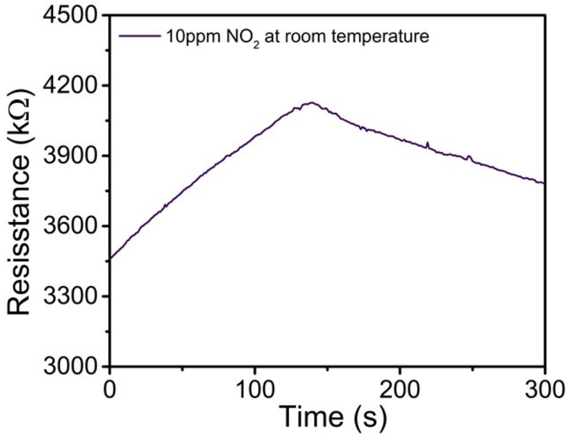

Supplementary Figure S6. Room temperature response-recovery cycle of the of 2D In_2O_3 in 10 ppm NO_2.

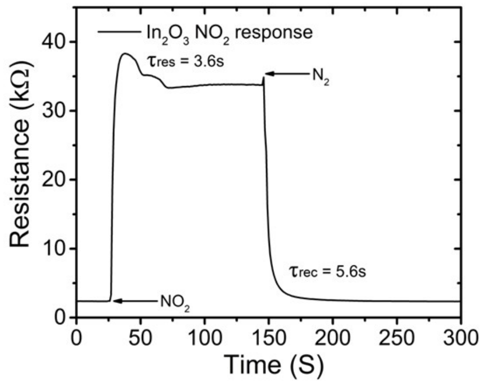

Supplementary Figure S7. The steady-state response-recovery cycle of 2D In_2O_3 gas sensor to 10 ppm NO_2 at 275 ^oC showing 1514 % response and 3.6 s and 5.6 response and recovery times, respectively.

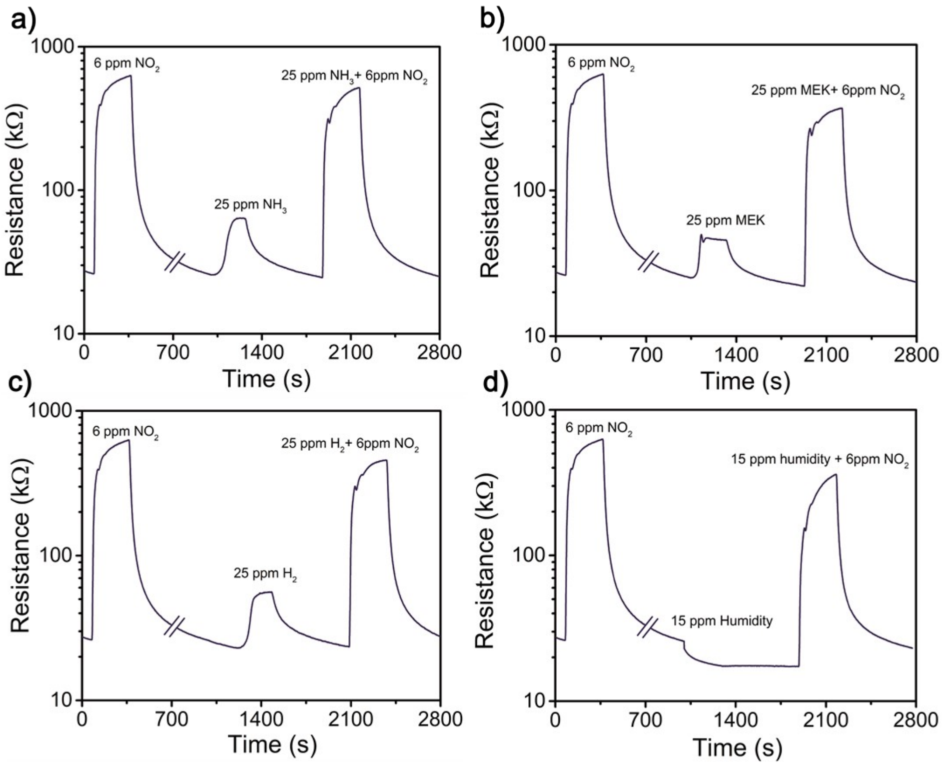

Supplementary Figure S8. Developed sensor's cross selectivity data at 200 ℃. **a**) 2D In_2O_3 gas sensor response to 25 ppm NH_3 (including 2.5% O_2) and NH_3 mixed with NO_2. **b**) 2D In_2O_3 gas sensor response to 25 ppm MEK (including 2.5% O_2) and MEK mixed with NO_2. **c**) 2D In_2O_3 gas sensor response to 25 ppm H_2 (include 2.5% O_2) and H_2 mixed with NO_2. **d**) 2D In_2O_3 gas sensor response to 15 ppm H_2O (include 2.5% O_2) and H_2O mixed with NO_2

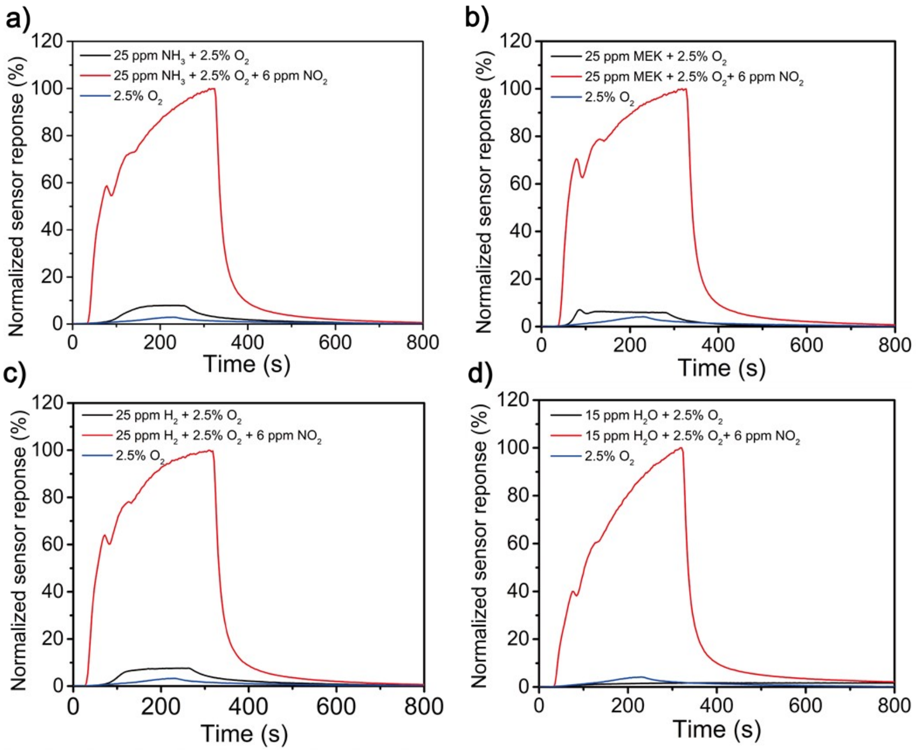

Supplementary Figure S9. Control experiments for cross-sensitivity analysis at 200 °, primarily to assess the effect of O_2 on the sensing mechanism for a)NH_3, b)MEK, c)H_2, and d)H_2O.

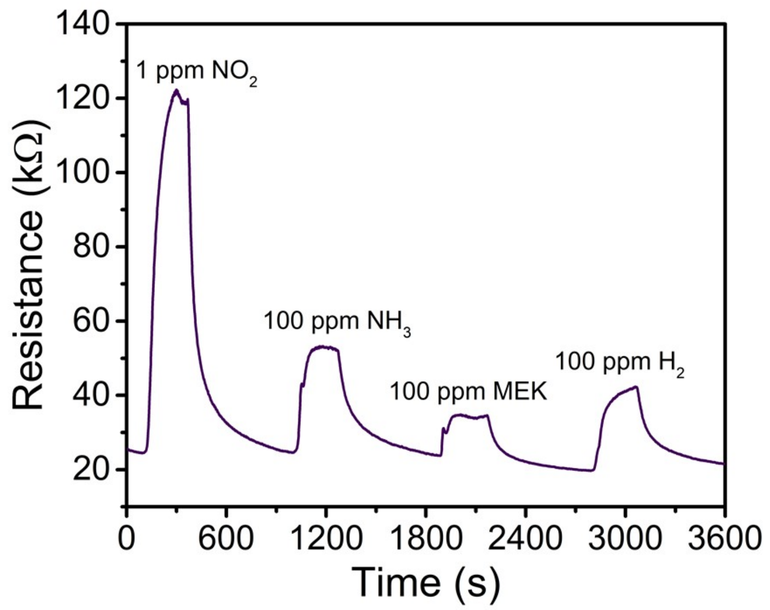

Supplementary Figure S10. Developed sensor's hysteresis data at 200 ℃.

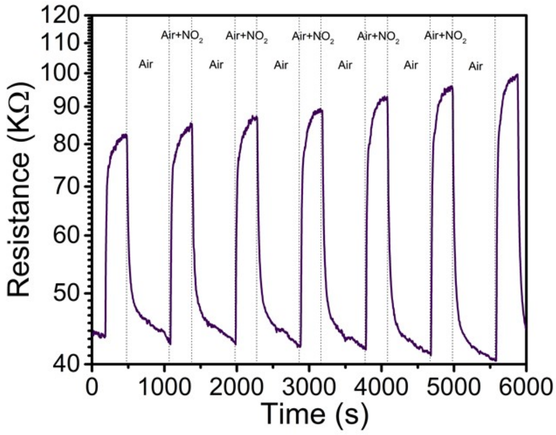

Supplementary Figure S11. Response of 2D In_2O_3 gas sensors to 10 ppm NO_2 in air.

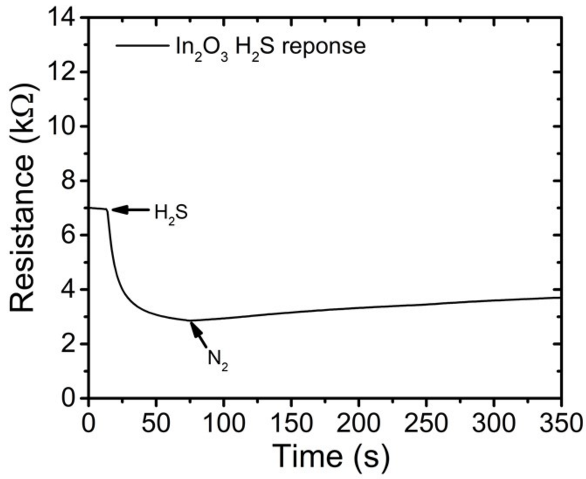

Supplementary Figure S12. Sensing performance of 2D In_2O_3 to 100 ppm H_2S showing irreversible gas sensing behavior.

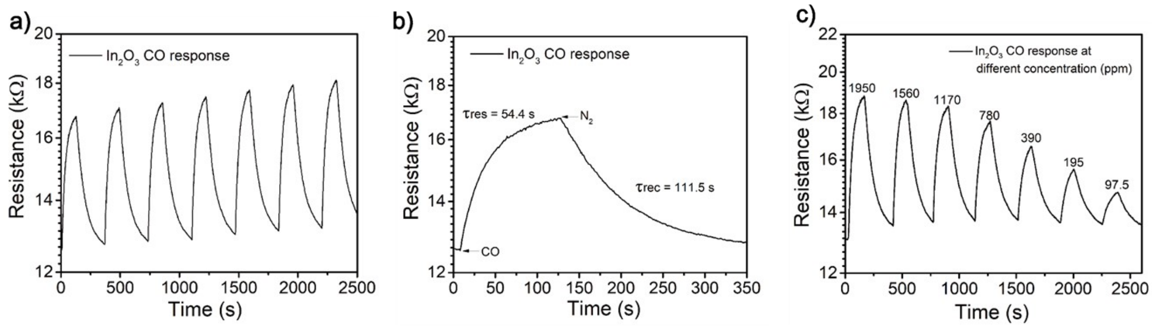

Supplementary Figure S13. a) Response and recovery cycles of In_2O_3-based gas sensors to 1950 ppm CO at 200 ℃. b) Single response and recovery curve of In_2O_3-based gas sensors to 1950 ppm CO at 200 ℃. c) Repeated response and recovery curves of In_2O_3-based gas sensors to different concentrations of CO at 200 ℃.

Supplementary Table 1. Comparison of nanoscale In_2O_3-based gas sensors for nitrogen dioxide detection with different morphologies recently reported in the literature.

Sensing materials	Morphology	Temperature (°C)	Response (%)	Response time (s)	NO_2 detected (ppm)	Limit of detection (ppm)	Ref
In_2O_3	Nanosheets	RT	89.48	16.6	97	-	1
In_2O_3	Nanosheets	120	213	4	10	0.01	2
In_2O_3	Microcubes	100	1401	16	100	-	3
In_2O_3	Microcubes	60	1884	-	30	2	4
In_2O_3	Microcubes	100	336	18	100	0.001	5
In_2O_3	Nanoparticles	300	1.09	120	3	-	6
In_2O_3	Nanosheets	250	164	5	50	-	7
In_2O_3	Nanorods	80	82	70	2	0.1	8
Sn/ In_2O_3	Nanofibers	90	44.6	106	1	-	9
Pd/ In_2O_3	Nanosheets	110	4080	120	50	0.5	9
Pd/ In_2O_3	Nanowires	300	3.4	60	30	-	10
Graphene/ In_2O_3	Nanofiber	50	42	261	5	0.00086	11
Ti/ In_2O_3	Thin films	400	16.95	-	0.080	-	12
This work	2D sheets	RT	55	>150 s	10	-	
This work	2D sheets	200	1974	76	10	0.004	
This work	2D sheets	275	1514	3.6	10	-	

Reference

1. L. Sun, W. C. Fang, Y. Yang, H. Yu, T. T. Wang, X. T. Dong, G. X. Liu, J. X. Wang, W. S. Yu and K. Y. Shi, *Rsc Advances*, 2017, **7**, 33419-33425.
2. X. Wang, J. Su, H. Chen, G. D. Li, Z. Shi, H. Zou and X. Zou, *ACS Appl. Mater. Interfaces*, 2017, **9**, 16335-16342.
3. K. K. Pawar, J. S. Shaikh, S. S. Mali, Y. H. Navale, V. B. Patil, C. K. Hong and P. S. Patil, *J Alloy Compd*, 2019, **806**, 726-736.
4. S. T. Navale, C. Liu, Z. Yang, V. B. Patil, P. Cao, B. Du, R. S. Mane and F. J. Stadler, *J Alloy Compd*, 2018, **735**, 2102-2110.
5. Z. J. Li, S. N. Yan, M. X. Sun, H. Li, Z. L. Wu, J. Q. Wang, W. Z. Shen and Y. Q. Fu, *J Alloy Compd*, 2020, **816**.
6. P. S. Khiabani, E. Marzbanrad, H. Hassani and B. Raissi, *J Am Ceram Soc*, 2013, **96**, 2493-2498.
7. L. P. Gao, Z. X. Cheng, Q. Xiang, Y. Zhang and J. Q. Xu, *Sensor Actuat B-Chem*, 2015, **208**, 436-443.
8. W. J. Du, W. X. Si, J. B. Zhao, F. L. Wang, Z. J. Han, Z. Wang, W. Liu, G. X. Lu, J. R. Liu and L. L. Wu, *Ceram Int*, 2020, **46**, 20385-20394.
9. J. S. Ri, X. W. Li, C. L. Shao, Y. Liu, C. H. Han, X. H. Li and Y. C. Liu, *Sensor Actuat B-Chem*, 2020, **317**.
10. S. S. Kim, J. Y. Park, S.-W. Choi, H. G. Na, J. C. Yang and H. W. Kim, *J Alloy Compd*, 2011, **509**, 9171-9177.
11. C. Yan, H. B. Lu, J. Z. Gao, Y. Zhang, Q. M. Guo, H. X. Ding, Y. T. Wang, F. F. Wei, G. Q. Zhu, Z. B. Yang and C. L. Wang, *J Alloy Compd*, 2018, **741**, 908-917.
12. L. G. Bloor, J. Manzi, R. Binions, I. P. Parkin, D. Pugh, A. Afonja, C. S. Blackman, S. Sathasivam and C. J. Carmalt, *Chemistry of Materials*, 2012, **24**, 2864-2871.